Heliyon 10 (2024) e31037

Contents lists available at ScienceDirect

Heliyon

journal homepage: www.cell.com/heliyon

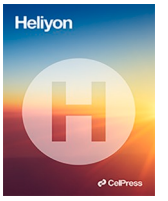

Research article

Influence of overlay strength degradation on bond stresses of bridge deck system

Rajai Z. Al-Rousan *, Bara'a R. Alnemrawi

Department of Civil Engineering, Engineering, Jordan University of science and technology, P.O. Box 3030, Irbid 22110, Jordan

ARTICLE INFO

Keywords:
Overlay
Degradation
Thickness
Bond strength
NLFEA
Live load
Shrinkage

ABSTRACT

This research paper intends to numerically investigate the impact of selected factors on the strength of the concrete overlay-bridge deck bond, directly and indirectly, using the nonlinear finite element analysis (NLFEA) method. Besides, the research introduces the guidelines necessary to attain adequate bond strength to eliminate the possibility of concrete detachment under the effect of different developed stresses. The NLFEA has been utilized in predicting and correlating the live applied loads and the induced shrinkage stresses at the interfacial region between the concrete overlay and the bridge deck. The developed stresses were related to the overlay's direct tensile bond strength. A total of 336 NLFEA models of overlay-bridge deck slab segments were designed and examined after being properly validated. The parameters of the study were as follows: the overlay degradation level (0 %, 19 %, 36 %, 51 %, 64 %, and 75 %); the ratio of the overlay's relative thickness-to-the bridge deck slab ($t_{overlay}/t_{slab}$); in addition to the age of the shrinkage induced stresses (early age (3 and 7 days) and moderate age (14 and 28 days)). The NLFEA live load and shrinkage stress values were validated using experimental results from the literature with difference percentages of less than 5 %. The numerical study results recommended that the thickness of the concrete's overlay should be within certain overlay thickness limits to be capable of handling the lower and higher stresses at the service and overloading conditions. The proposed guidelines enable the avoidance of unfavorable detachment between the interface parts under the effect of AASHTO HS-20 truck cyclic and impact loadings, as well as shrinkage loading.

1. Introduction

Bridge deck concrete decks are subjected to a high risk of concrete cracking and reinforcement corrosion during their service life, especially under dynamic vehicular loads and environmental conditions [1–4]. Improving the structural performance using the bonded overlay either to rehabilitate or strengthen the original bridge deck system [5]. Conventional cement-based or latex-based materials, such as the normal-strength concrete are not enough to secure the service life of the bridge deck [6]. The serviceability of the bridge deck-overlaying layer interface is highly dependent on the bond strength at the interface region. However, stresses are induced as a result of the motion between the two connected parts [7–10]. The interface location exhibited complicated stress conditions, as these stresses are affected, directly and indirectly, by several factors.

The induced stresses at the interfacial bond between the bridge deck and the overlay start to appear at the instant when the concrete overlay is placed on the bridge deck till the overlay gains the proper bond strength and the live load is applied. When the overlay is

* Corresponding author.
E-mail addresses: rzalrousan@just.edu.jo (R.Z. Al-Rousan), bralnemrawi19@eng.just.edu.jo (B.R. Alnemrawi).

https://doi.org/10.1016/j.heliyon.2024.e31037
Received 25 September 2023; Received in revised form 8 May 2024; Accepted 9 May 2024
Available online 10 May 2024

constructed at the top of the bridge deck, the overlay encounters drying shrinkage, which begins just after the moist curing is completed. The substrate beneath the bridge deck constrains the shrinkage of the overlay, leading to the development of stresses within the bond [11–13]. Standardly, the bridge deck can be made of precast and cast-in-place concrete parts that are connected, interact, and develop their full strength before the placing of an overlaying layer where the possibility of drying shrinkage is almost avoided.

The concrete overlay shrinks quickly in the first 1–7 days. Then, the shrinking rate reduces to 28 days when the shrinkage rate becomes at its lowest value. The induced shrinkage stresses, at 1–7 days (early) age, have a significant influence and can cause the overlay to detach at an early age. After this crucial time interval, the majority of shrinkage strains are mitigated by the relaxation process. Often, the live load is not to be applied unless the overlay gains the required level of bond strength. Further, placing the overlay on the entire deck surface likely minimizes the level of mechanical loading stresses at the concrete's overlay-substrate interface, but the concrete bridge deck's surface encounters cracks in some places [14]. A few research studies have been carried out to investigate the stresses within the deck-overlay interface. For example, Delatte and Sehdev [15] found that the strength of the bond enhanced at the age of 1–3 days, but the enhancement rate was much less at the age of 7 and 14 days. In another study, Babaei [16] revealed that the LMC overlay had a stronger bonding than the ones made of low-slump dense concrete (LSDC). Also, Wells et al. [17] research estimated that an adequate 28-day-aged bond strength's value should be 0.90 MPa, at least. In addition, Sprinkel and Ozyildirim [18] considered that the bond strength value of 1.38 MPa at 28 days after the construction was good, while the 2.06 MPa was excellent.

The utilization of ultra-high strength concrete (UHPC) is a good choice for upgrading the system performance due to its high mechanical and durability properties [19,20]. Thin bonded UHPC was efficiently utilized for rehabilitating the bridge deck in the literature [21] where the thickness of the overlay varies between 35 mm and 50 mm. Based on the literature results, the UHPC can effectively extend the service life of the bridge deck. Generally, the flexural capacity of the UHPC composite decks depends on many factors, including the strengthening configuration [22], the existence of reinforcement in the overlay layer [23], the mechanical properties of the UHPC material [24], the bond at the concrete bridge deck [25], and UHPC materials, and the overlay thickness [26].

Moreover, Patricia et al. [27] recommended that the overlay's bond strength after 28 days, whether made of LMC or MSC, should be a minimum of 1.03 MPa. Also, a study by Bernard [28] found that the development and severity of the overlay's delamination were governed by the thickness ratio in old and fresh layers of concrete and the interface's tensile strength. Further, Issa et al. [29] used NLFEA to numerically investigate the behavior of a full-depth precast concrete bridge deck panel system prior to and post-overlaying with different types of overlays made of plain and fibrous LMC and MSC. The NLFEA models were validated with the previously published experimental research data related to the subject of the study. In addition, Fowler [30] presented a set of guidelines to compute the value of the heat-induced stresses at the concrete's overlay-substrate interface. In the presence of a concrete overlay, the relative thermally induced stresses at the interface location were minimal due to the close thermal expansion coefficients between the concrete slab and the overlay layer material [30,31]. While the concrete overlay layer delaminates if the bond stresses are higher than the overlay's bond strength.

Bridge is an essential and sensitive structure exposed to different loading and environmental conditions resulting in degrading their ability to sustain the service loads. However, many components composed the structural system such as the stringers, girders, and decks. The bridge deck slabs play a major role in distributing the induced traffic loads to piers. The aging and continuous loadings decrease the ability of the bridge system to sustain loading and increase the need for strengthening or rehabilitation. The method of bridge overlaying method proved to be an efficient method that remains functional and serviceable for up to 30 years. Therefore, the present research paper tries to accomplish several goals: (a) investigating and analyzing the strength of the bridge deck-overlay bond in a bridge deck, considering: i) various levels of overlay's degradation in strength, ii) the ratio of overlay's thickness-to-the bridge deck slab ($t_{overlay}/t_{slab}$), and iii) the age of the induced-by-shrinkage stresses; and (b) adequate guidelines regarding the strength of bond required for concrete not to delaminate when at different stress levels.

2. Nonlinear finite element analysis (NLFEA)

2.1. General

The ANSYS V.15 [32] software was used to examine the bond strength between the concrete bridge deck and overlay layer with (200 × 200 mm) dimension block. The modeling parameters are illustrated in Table 1. The study parameter of $t_{overlay}/t_{slab}$ ratio was set as (0.03, 0.06, 0.09, 0.12, 0.15, 0.18, 0.21, 0.24, 0.27, 0.30, 0.33, 0.36, 0.39, and 0.42) corresponding to overlay's thickness (6, 12, 18, 24, 30, 36, 42, 48, 54, 60, 66, 72, 78, and 84) mm, respectively, with a fixed slab's thickness (t_{slab}) of 200 mm (Table 1). Additionally, every $t_{overlay}/t_{slab}$ ratio was tested under six different degradation levels in the overlay's strengths (0 %, 19 %, 36 %, 51 %, 64 %, and

Table 1
Investigated parameters for simulated NLFEA models ($f'_{c,\ slab}$ of 50 MPa and t_{slab} of 200 mm).

Variables	Applied Values
$t_{overlay}/t_{slab}$	0.03 (6 mm), 0.06 (12 mm), 0.09 (18 mm), 0.12 (24 mm), 0.15 (30 mm), 0.18 (36 mm), 0.21 (42 mm), 0.24 (48 mm), 0.27 (54 mm), 0.30 (60 mm), 0.33 (66 mm), 0.36 (72 mm), 0.29 (78 mm), and 0.42 (84 mm)
Overlay strength degradation level, %	0 %, 19 %, 36 %, 51 %, 64 %, and 75 %
Shrinkage age, Days	3 days, 7 days, 14 days, and 28 days

75 %). The resulted in (84) various study cases, each of which had four shrinkage stress ages (early ages of 3 and 7 days and moderate ages of 14 and 28 days). Therefore, the total NLFEA models were 336, with the selected parameter values illustrated in Table 1 based on the available literature and previous experience.

2.2. Material and elements

The SOLID65 element was utilized in modeling the overlay and bridge deck with the steel disk modeled using the eight-node SOLID45 element. However, the SOLID65 ANSYS element could predict the concrete's nonlinear performance by employing the smeared cracking approach. Hence, it was possible to determine a criterion for concrete failure under multi-axial stress using the model established by William and Warnke [33] with the concrete's Poisson ratio set at 0.2. The value of the shear transfer coefficient (β_t), which denoted the crack surface's states, was employed by many research related to RC structures [34–37]. Specifically, the value of β_t was selected as 0.2 where the range of the β_t factor according to Hemmaty [38] is equal to $0.05 - 0.25$. The concrete bridge deck and the overlay layer were initially assumed to have an equal compressive strength property of 50 MPa modeled using the Kent and Park model [39] for modeling the stress-strain behavior of the concrete material, as shown in Fig. 1. However, the degradation in the overlay layer strength was one of the parameters studied in this research where the degradation was a percent of the original compressive strength (50 MPa) and reflected by reducing the concrete strength in the simulated models [40–42].

Half of the bridge deck system with an overlaying layer is modeled according to the existing symmetry in the geometry and boundary condition. However, the model was analyzed using proper boundary conditions where a symmetry boundary condition has $U_z = 0$ and $UR_x = UR_y = 0$ for a face whose normal is parallel to the z-axis [43]. Fig. 2 illustrates the proper meshing for the FE models. Hypothetically, the strength of the concrete deck-steel disc and the bridge deck-overlay bonds should be considered. However, this research paper assumed the bonds were in perfect condition since no detachment was observed during the experimental testing. The bond strength of the bridge deck slab and the overlay layer is examined using the pull-off test. However, the test involves applying a direct tensile load to a partial core advanced through the overlay material and into the underlying concrete until failure occurs. The tensile load is applied to the partial core through the use of a metal disk with a pull pin, bonded to the overlay with an adhesive material [44–46].

The tensile loads were exerted, in a uniform manner, on the disc's top side as the disc was put on the overlay-bridge deck slab segment models. The values of the applied shrinkage strains were (105, 202, 339, and 426) με, corresponding to overlay's ages of (3, 7, 14, and 28) days [12] applied in the XY and ZY plains of the overlay layer (Fig. 2). The total applied load was split into several steps (increments) where the Newton–Raphson equilibrium iterations was utilized to ensure the solution convergence at the increments' ends, with a tolerance of 0.001. Upon the concrete cracking, the loading application was of a smaller size. Every one of the models encountered a failure when the solution for the load step of 0.0045 kN did not converge.

2.3. Validating the NLFEA models

The NLFEA models of the bond between the bridge deck slab and the overlay layer were validated using the experimental testing results done by Issa et al. [12] (Table 2) and Delatte et al. [15] (Table 3). The obtained results presented in Table 3 showed that the FEA's findings agreed well with the experimental bond strength values. All the obtained findings affirmed that the FEA modeled system well and accurately matched the properties of a realistic system. Making a comparison between the study made by Issa et al. [12] and the one made by Delatte et al. **[15]** in terms of bond strength, it was found that the whole mixes in the samples of Issa et al. **[12]** exhibited greater values of bond strength. In the same context, Fig. 3 demonstrates the FEA's induced shrinkage stresses, developed between the bridge deck and overlay, after being validated with experimentally-attained findings by Issa et al. **[12]** , Jonas Carlswärd

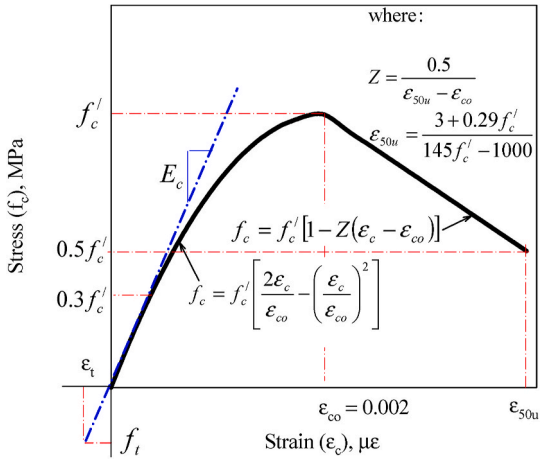

Fig. 1. Concrete stress-strain theoretical modeling [39].

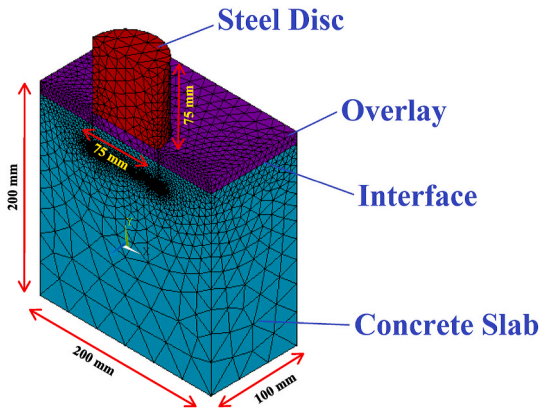

Fig. 2. Typical finite element meshing of Overlay-bridge deck slab segment of 200 × 200 mm.

Table 2
Issa et al. [12] Experimental direct tensile bond strength and NLFEA results.

Overlay Type		Shrinkage age, Days	Bond strength		Error, %
			Experimental, MPa	NLFEA, MPa	
Integral plain LMC overlay		14	3.30	3.35	1.5
		28	3.53	3.55	0.6
Cast-in-place	Plain	14	2.64	2.60	−1.5
LMC overlay	Synthetic		2.53	2.50	−1.2
	Steel		2.66	2.61	−1.9
	Plain	28	2.82	2.85	1.1
	Synthetic		2.74	2.78	1.5
	Steel		2.66	2.71	1.9
Cast-in-place	Plain	14	2.61	2.56	−1.9
MSC overlay	Synthetic		2.53	2.50	−1.2
	Steel		2.46	2.44	−0.8
	Plain	28	2.98	3.01	1.0
	Synthetic		2.87	2.89	0.7
	Steel		2.94	2.97	1.0

Table 3
Delatte et al. [15] experimental direct tensile bond strength and NLFEA results.

Overlay Type	Shrinkage age, Days	Bond strength		Error, %
		Experimental, MPa	NLFEA, MPa	
Mix 1 HP	1	0.81	0.77	−4.9
	3	1.04	1.00	−3.8
	7	1.84	1.87	1.6
	14	2.23	2.32	4.0
Mix 2 HF	1	1.00	0.95	−5.0
	3	1.51	1.46	−3.3
	7	2.36	2.41	2.1
	14	2.58	2.68	3.9
Mix 7 NFFA	1	0.63	0.59	−6.3
	3	1.34	1.30	−3.0
	7	1.65	1.68	1.8
	14	1.96	2.04	4.1

[47], and Shin and Lange [48]. Fig. 3 indicates that the FEA models' shrinkage values agreed, to a good extent, with the experimental models' shrinkage values. Therefore, the shrinkage of the FEA models was extended to investigate the influence of the study parameters (Table 1) on the induced shrinkage stresses between the bridge deck system and overlay in terms of normal stresses.

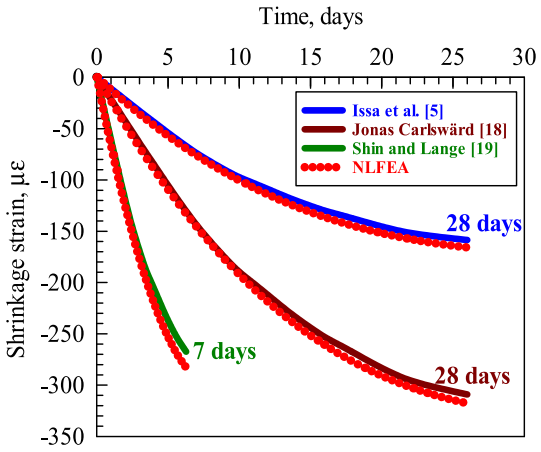

Fig. 3. Experimental shrinkage strain [12,47,48] and NLFEA at overlay-bridge deck slab interface.

3. Analysis results and discussions

3.1. Overlay bond strength

Issa [49] called for considering the strength value exceeding 2.06 MPa as excellent for direct bonds, the value of bond strength ranging between 1.72 and 2.06 MPa should be considered as very good, the values of bond strength ranging between 1.38 and 1.72 MPa to be considered as good, the values of bond strength between 0.69 and 1.38 MPa to be considered as fair, and the values of the bond strength between 0 and 0.69 MPa to be considered as poor. For every modeled sample, the strength values of the overlay-bridge deck bond were graphically represented against the ratio of $t_{overlay}/t_{slab}$ at the levels of the overlay strength degradation and at various ages of induced-by-shrinkage stresses (Fig. 4(a-f)). Inspection of Fig. 4(a-f) indicated that the FEA models' bond strength enhanced, in a rapid manner, to a specific ratio of $t_{overlay}/t_{slab}$ of 0.18 which met the overlay's thickness of 36 mm. At a $t_{overlay}/t_{slab}$ of 0.18, the FEA models' bond strength enhanced moderately. Therefore, the least recommended overlay thickness should be more than 36 mm. Besides, a recommendation was made to choose an overlay's thickness of at least 57 mm globally to avoid sneaking salt into concrete bridge decks **[12]**.

The overlay sample which had a strength degradation level of 0 % and an age of 28 days had a value of $t_{overlay}/t_{slab}$ of: larger than 0.065 (excellent), 0.053–0.065 (very good), 0.040–0.053 (good), and 0.040–0.030 (fair) (Fig. 4(a)). Also, the overlay's strength degradation level of 0 % and 14 days, for $t_{overlay}/t_{slab}$ of higher than 0.075, 0.056 to 0.075, 0.045 to 0.056, and 0.045 to 0.030 could be categorized as: excellent, very good, good, and fair bond strength criteria, respectively (Fig. 4(a)). For 7 days-aged samples with a strength degradation level of 0 %, the $t_{overlay}/t_{slab}$ of greater than 0.105, 0.074 to 0.105, 0.053 to 0.074, and 0.053 to 0.030 could be categorized as: excellent, very good, good, and fair bond strength, respectively. As for the overlay samples with a strength degradation level of 0 % and 3 days of age, the $t_{overlay}/t_{slab}$ of 0.420, 0.140 to 0.420, 0.075 to 0.140, 0.075 to 0.035, and 0.035 to 0.030 could be classified as: excellent, very good, good, fair, and poor bond strength, respectively (Fig. 4(a)).

As for the overlay specimens with a strength degradation level of 19 % and 28 days of age, the $t_{overlay}/t_{slab}$ of greater than 0.075, 0.058 to 0.075, 0.044 to 0.058, and 0.044 to 0.030 could be classified as: excellent, very good, good, and fair bond strength, respectively (Fig. 4(b)). The overlays with a strength degradation level of 19 % and 14 days of age had a $t_{overlay}/t_{slab}$ of: higher than 0.088, 0.066 to 0.088, 0.050 to 0.066, and 0.050 to 0.030 could be classified as: excellent, very good, good, and fair bond strength, respectively. The overlay samples with a strength degradation level of 19 % and 7 days of age had a $t_{overlay}/t_{slab}$ of over 0.150, 0.089 to 0.150, 0.058 to 0.089, and 0.058 to 0.031, which could be classified as: excellent, very good, good, and fair bond strength, respectively (Fig. 4(b)). The overlay specimens with a strength degradation level of 19 % and 3 days of age had a $t_{overlay}/t_{slab}$ of 0.223–0.420, 0.089 to 0.223, 0.089 to 0.040, and 0.040 to 0.030, which could be classified as: very good, good, fair, and poor bond strength, respectively (Fig. 4(b)).

Additionally, the overlay specimens with a strength degradation level of 36 % and 28 days of age had a $t_{overlay}/t_{slab}$ of greater than 0.094, 0.068 to 0.094, 0.050 to 0.068, and 0.050 to 0.030, which could be classified as: excellent, very good, good, and fair bond strength, respectively (Fig. 4(c)). The samples of overlays with a strength degradation level of 36 % and 14 days of age had a $t_{overlay}/t_{slab}$ of greater than 0.120, 0.079 to 0.120, 0.055 to 0.079, and 0.055 to 0.030, which could be classified as: excellent, very good, good, and fair bond strength, respectively (Fig. 4(c)). The overlays with a strength degradation level of 36 % and 7 days of age had a $t_{overlay}/t_{slab}$ of greater than 0.270, 0.120 to 0.270, 0.069 to 0.120, 0.069 to 0.033, and 0.033 to 0.030, which could be classified as: excellent, very good, good, fair, and poor bond strength, respectively (Fig. 4(c)). The overlays with a strength degradation level of 36 % and 3 days of age had a $t_{overlay}/t_{slab}$ of 0.120–0.420, 0.042 to 0.120, and 0.042 to 0.030, which could be classified as: good, fair, and poor bond strength, respectively (Fig. 4(c)).

The overlays with a strength degradation level of 51 % and 28 days of age had a $t_{overlay}/t_{slab}$ of higher than 0.144, 0.085 to 0.144, 0.058 to 0.085, and 0.058 to 0.030, which could be classified as: excellent, very good, good, and fair bond strength, respectively (Fig. 4

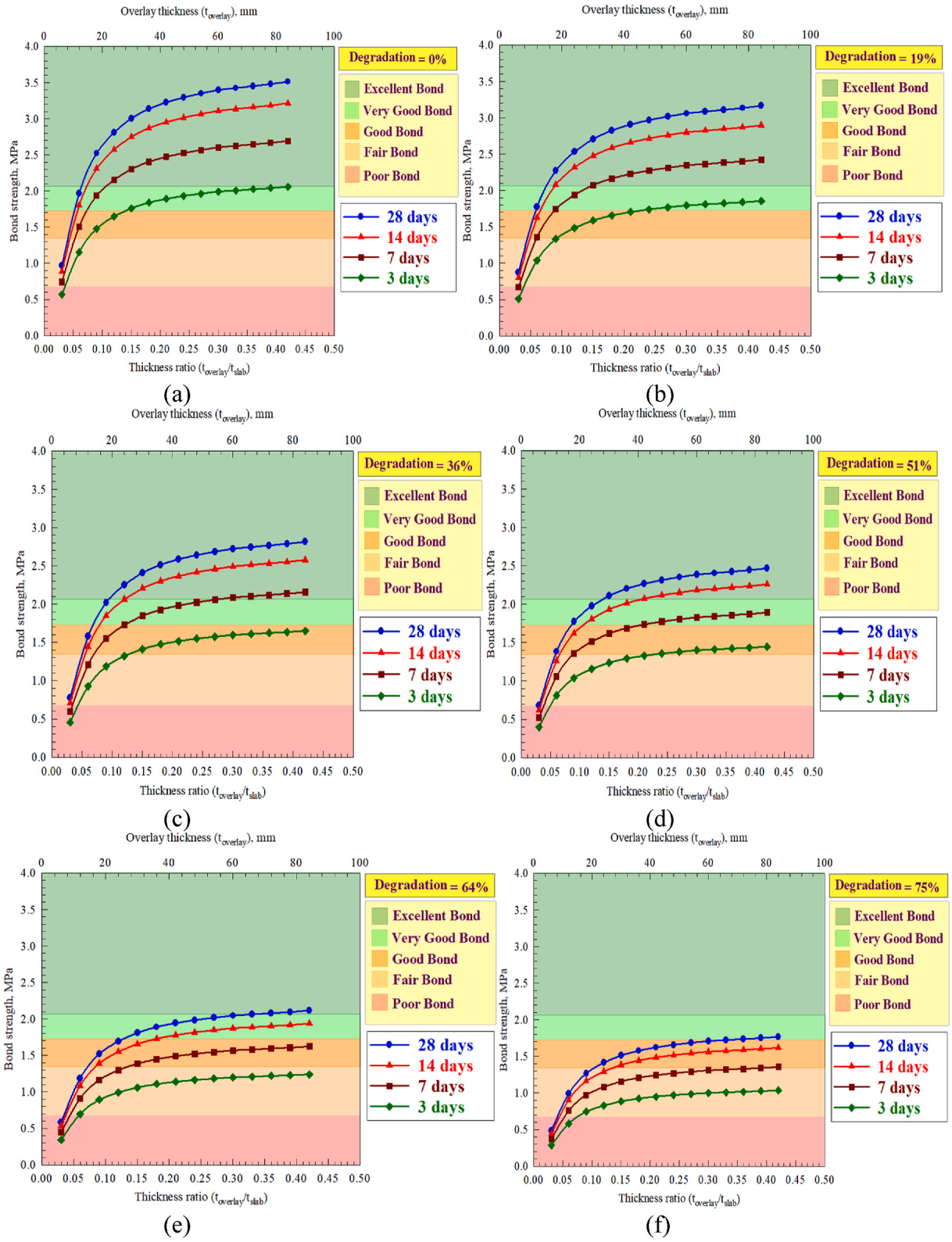

Fig. 4. Bond strength versus investigated parameters for different degradation levels (a) 0 %, (b) 19 %, (c) 36 %, (d) 51 %, (e) 64 %, and (f) 75 %.

(d)). The overlays with a strength degradation level of 51 % and 14 days of age had a $t_{overlay}/t_{slab}$ of higher than 0.210, 0.107 to 0.210, 0.065 to 0.107, 0.065 to 0.033, and 0.033 to 0.030, which could be classified as: excellent, very good, good, fair, and poor bond strength, respectively (Fig. 4(d)). The overlays with a strength degradation level of 51 % and 7 days of age had a $t_{overlay}/t_{slab}$ of

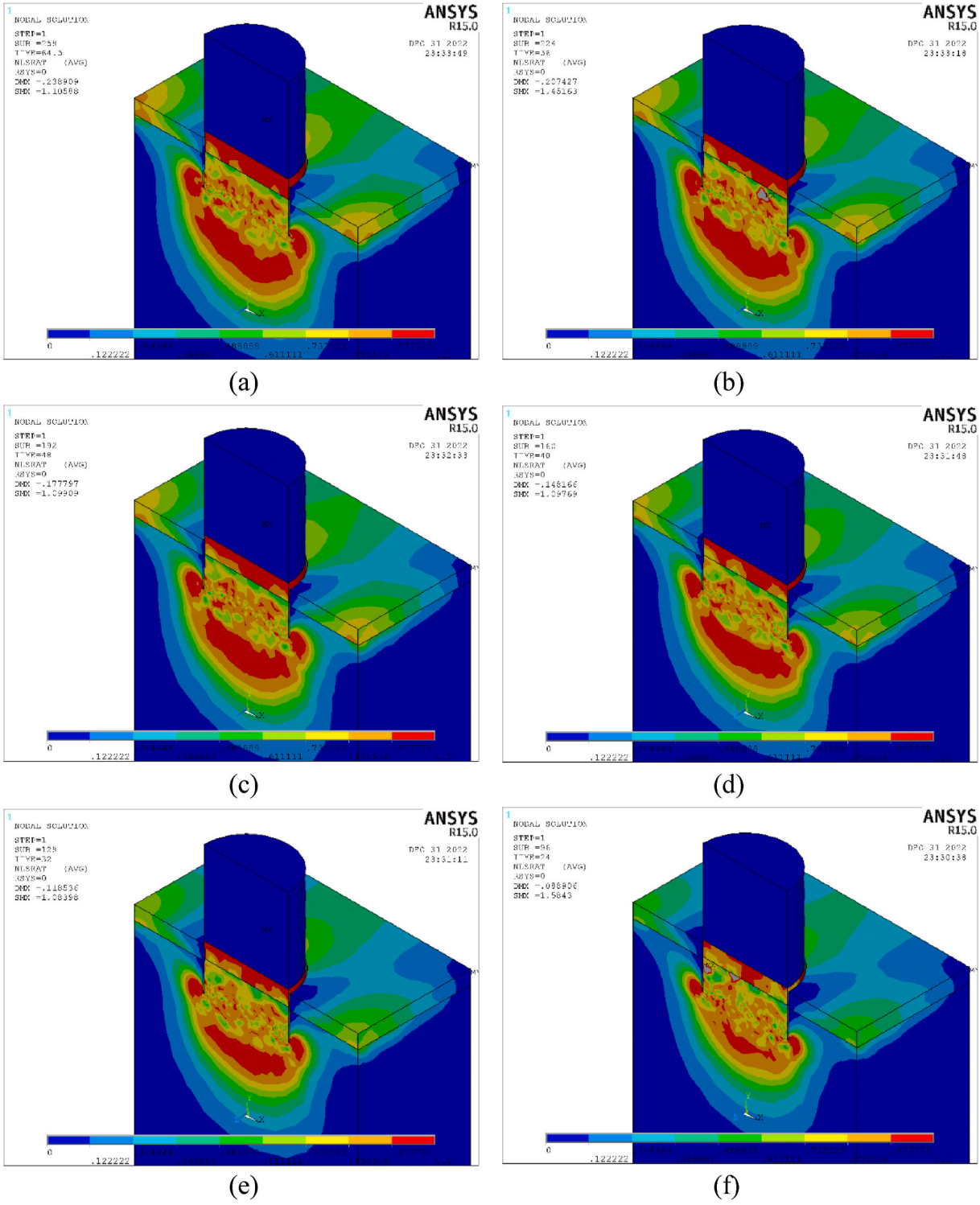

Fig. 5. The typical stress ratio if model with overlay $t_{overlay}/t_{slab}$ of 0.03 for different degradation levels (a) 0 %, (b) 19 %, (c) 36 %, (d) 51 %, (e) 64 %, and (f) 75 %.

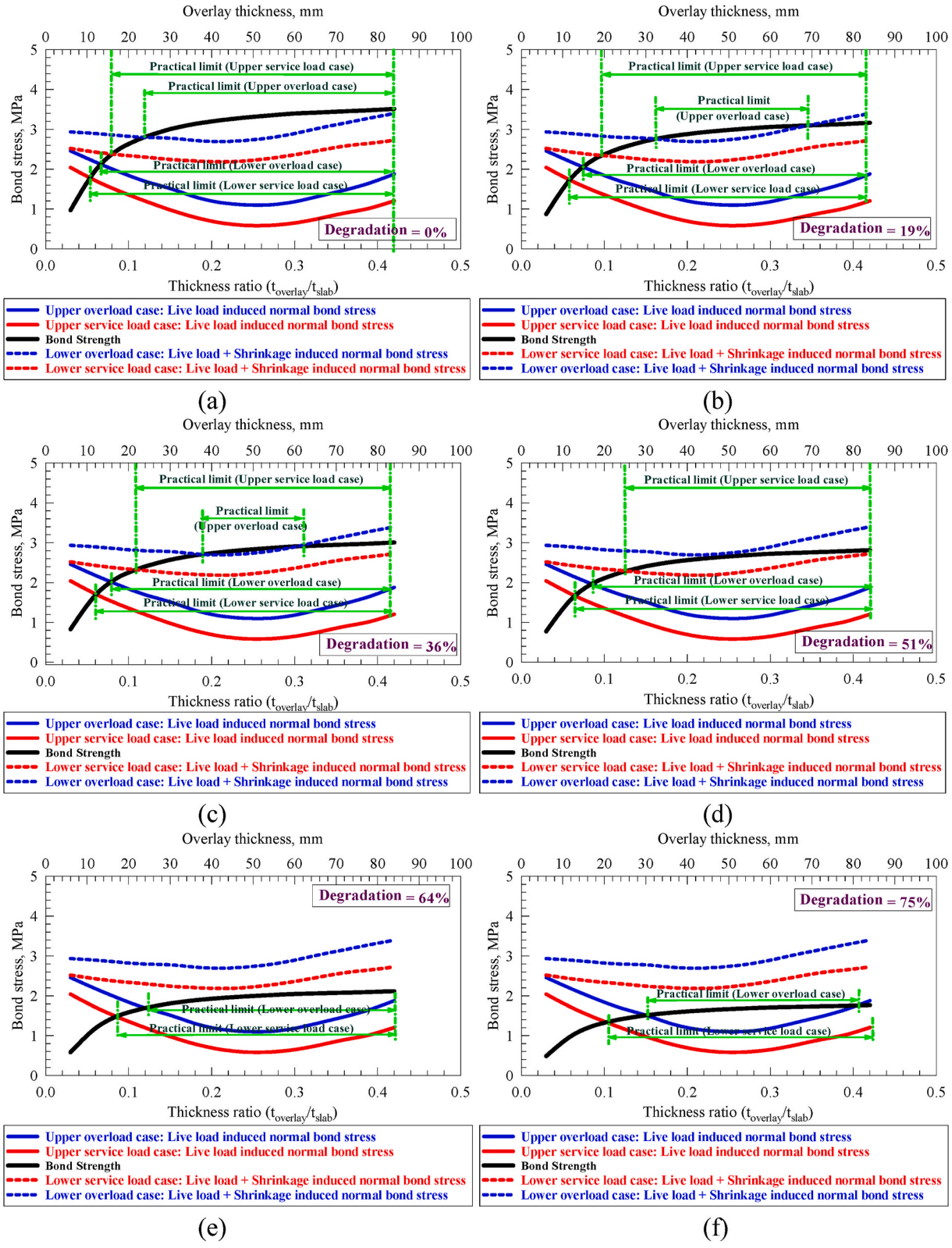

Fig. 6. Live load and shrinkage induced normal bond stresses versus overlay thickness ratio for different degradation levels (a) 0 %, (b) 19 %, (c) 36 %, (d) 51 %, (e) 64 %, and (f) 75 %.

0.210–0.420, 0.085 to 0.210, 0.085 to 0.037, and 0.037 to 0.030, which could be classified as: very good, good, fair, and poor bond strength, respectively (Fig. 4(d)). The overlays with a strength degradation level of 51 % and 3 days of age had a $t_{overlay}/t_{slab}$ of 0.210–0.420, 0.050 to 0.210, and 0.050 to 0.030, which could be classified as: good, fair, and poor bond strength, respectively (Fig. 4 (d)).

The overlays with a strength degradation level of 64 % and 28 days of age had a $t_{overlay}/t_{slab}$ of higher than 0.330, 0.126 to 0.330, 0.072 to 0.126, 0.072 to 0.033, and 0.033 to 0.030, which could be classified as: excellent, very good, good, fair, and poor bond strength, respectively (Fig. 4(e)). The overlays with a strength degradation level of 64 % and 14 days of age had a $t_{overlay}/t_{slab}$ of 0.186–0.420, 0.084 to 0.186, 0.039 to 0.084, and 0.039 to 0.030, which could be classified as: very good, good, fair, and poor bond strength, respectively (Fig. 4(e)). The overlays with a strength degradation level of 64 % and 7 days of age had a $t_{overlay}/t_{slab}$ of 0.136–0.420, 0.045 to 0.136, and 0.045 to 0.030, which could be classified as: good, fair, and poor bond strength, respectively (Fig. 4 (e)). The overlays with a strength degradation level of 64 % and 3 days of age had a $t_{overlay}/t_{slab}$ of 0.063–0.420 and 0.063 to 0.030, which could be classified as: fair and poor bond strength, respectively (Fig. 4(e)).

The overlays with a strength degradation level of 75 % and 28 days of age had a $t_{overlay}/t_{slab}$ of 0.330–0.420, 0.106 to 0.330, 0.040 to 0.106, and 0.040 to 0.030, which could be classified as very good, good, fair, and poor bond strength, respectively (Fig. 4(f)). The overlays with a strength degradation level of 75 % and 14 days of age had a $t_{overlay}/t_{slab}$ of 0.137–0.420, 0.043 to 0.137, and 0.043 to 0.030, which could be classified as good, fair, and poor bond strength, respectively (Fig. 4(f)). The overlays with a strength degradation level of 75 % and seven days of age had a $t_{overlay}/t_{slab}$ of 0.350–0.420, 0.350 to 0.053, and 0.053 to 0.030, which could be classified as good, fair, and poor bond strength, respectively (Fig. 4(f)). The overlays with a strength degradation level of 75 % and three days of age had a $t_{overlay}/t_{slab}$ of 0.074–0.420 and 0.074 to 0.030, which could be classified as: fair and poor bond strength, respectively (Fig. 4(f)).

Fig. 5(a-f) exhibits the standard stress ratio in the overlay with a $t_{overlay}/t_{slab}$ of 0.03. The stress ratio could be defined as the ratio of the stress amount to the permitted stress allowed by the code related to the substance. This ratio ranges from 0 to 1.0, known as the least stress-to-highest stress. Inspecting Fig. 5 (a-f) indicated that the area of the stress ratio enhanced when the overlay's level of strength degradation was reduced.

3.2. Overlay thickness versus live load-induced bond stresses

The influence of the overlay's thickness on the structural behavior of the system's performance and the induced live loading bond stresses was studied [12,14]. The most observed case was when the overlay was put on a bridge deck with cracking. Such a case was employed to investigate the impact of the overlay's thickness on the induced live loading stresses. For every one of the modeled specimens, the overlay thickness's impact on the induced live loading bond stresses, normal and in shear, was studied under overloads and service loads (Fig. 6(a-f)). Inspecting Fig. 6(a-f) indicated that the induced live loading normal stresses against overlay's thickness could be split to three phases: the first phase, where the induced live loading normal stresses swiftly reduced, and continued up till the $t_{overlay}/t_{slab}$ became 0.18, corresponding to an overlay's thickness of 36 mm, after which the stresses reduced with a moderate rate up till the $t_{overlay}/t_{slab}$ was 0.33, corresponding to an overlay's thickness of 66 mm, in the second phase. Later, the induced live loading normal stresses commenced enhancing, as elaborated in the third phase. This finding is of great importance and has to be considered when planning to devise a concrete overlay with the best-fit thickness to resist different loading levels and harsh environmental conditions. Also, Fig. 6(a-f) indicated that the induced shrinkage and live loading stresses were almost 1.19, 1.33, 1.48, 1.65, 1.84, 2.09, 2.31, 2.46, 2.52, 2.45, 2.29, 2.14, 1.99, and 1.81. These readings were 1.19 (the least) to 2.52 (the highest) times the normal stresses at a $t_{overlay}/t_{slab}$ of 0.03, 0.06, 0.09, 0.12, 0.15, 0.18, 0.21, 0.24, 0.27, 0.30, 0.33, 0.36, 0.39, and 0.42, respectively. These values are in line with most previously published research [12,14,49].

Table 4
Practical limit for service and overload cases.

Degradation level, %	Load Case	Upper Limit		Lower Limit	
		Minimum, mm	Maximum, mm	Minimum, mm	Maximum, mm
0	Overload	24	84	13	84
	Service	16	84	11	84
19	Overload	32	69	14	84
	Service	19	84	12	84
36	Overload	36	66	15	84
	Service	22	84	13	84
51	Overload	NA	NA	17	84
	Service	25	84	14	84
64	Overload	NA	NA	25	84
	Service	NA	NA	16	84
75	Overload	NA	NA	32	82
	Service	NA	NA	20	84
Recommended for degradation level of less than 36 %	Overload	36	66	15	84
	Service	22	84	13	84
Recommended for degradation level of more than 36 %	Overload	NA	NA	32	82
	Service	NA	NA	20	84

3.3. Practical limit for overlay thickness to avoid debonding

Given a certain age and a level of strength degradation, the NLFEA results could be of much help in determining the most proper lower and upper size of an overlay, enough to provide the required resistance to live loading as well as shrinkage-induced stresses at the bonding region. Fig. 6(a-f) presents the values of the exerted live loading and shrinkage-induced normal stresses plotted against the bond's direct tensile strength. Additionally, Table 4 presents the actual limits of the cases of service loads and overloads that have been specified in Fig. 6(a-f). Table 4 indicated that the values of live loads and shrinkage induced normal stresses (the upper limit) in a degradation level less than 36 % were below the values of the bond's direct tensile strength in the models that had an overlay's thickness below 36 mm and higher than 66 mm in the overloading case. In addition, the same was observed at the service loading condition in a slab with an overlay thickness of less than 22 mm.

However, for the models under a live load only, the induced live loading normal stresses (lower limit) in a degradation level of less than 36 % were below the values of the bond's direct tensile strength in the models that had an overlay's thickness below 15 mm in the overloading case. In addition, the same was observed at the service loading condition in a slab with an overlay thickness of less than 13 mm. The simulated models, with an overlay's degradation level exceeding 36 %, had un-applicable least and highest overlay thicknesses because both the live load and shrinkage-induced normal stresses (the upper limits) exceeded the bond's direct tensile strength, causing a detachment of the overlay.

The induced normal stresses by the applied live loading with a degradation level of less than 36 % were less than the lower limits and below the values of the bond's direct tensile strength for the overloading cases of overlay thickness less than 32 mm or exceeding 82 mm. In addition, the same was observed at the service loading condition in a slab with an overlay thickness of less than 20 mm. As a result, the overlay thickness effectively enhances the shrinkage normal and shear stresses and reduces the induced live loading normal and shear stresses at the bond location. These stresses must be limited at all times by providing an overlay with a greater bond strength to eliminate the possibility of delamination.

As a result, it is unrecommended to use an overlay with a thickness exceeding 66 mm and below 36 mm for the models having an overlay degradation level $\leq$36 % (higher limit) because the overlay was prone, to a far extent, to be debonded and the bond's quality of the bridge deck with an overlaying layer could be at risk because of the enhancement in thickness. Also, the level of the overlay's degradation exceeding 36 % was not viable to be selected as a higher limit. It was found that this thickness was viable as a lower limit only where the overlay's thickness was below 32 mm and higher than 82 mm in the case of overload and for the models with an overlay's thickness below 20 mm in the case of service load.

4. Summary and conclusions

In the present research paper, bridge deck slabs with overlaying layer segments were modeled utilizing the NLFEA, with 200$\times$ 200 mm dimensions. The study parameters were the overlay's level of strength degradation, the ratio of $t_{overlay}/t_{slab}$, and the age of the shrinkage-induced stresses. The obtained findings have led to the following main conclusions:

1) The specimens with an overlay's level of degradation $\leq$36 % (higher limit) had an actual limit for $t_{overlay}/t_{slab}$ of 0.18–0.33, which corresponded to an overlay's thickness of 36–66 mm. The value of the overlay's thickness should not be higher than 66 mm or below 36 mm. That was because the overlay would be greatly prone to detachment, and the overlay-bridge deck bond's quality would be in jeopardy due to the enhancement in thickness. The caused-by-shrinkage shear stresses in the bond enhanced, at a rapid rate, to a $t_{overlay}/t_{slab}$ of 0.18, corresponding to an overlay's thickness of 36 mm; then, the enhancement rate became moderate.
2) As for the specimens with an overlay's level of degradation higher than 36 % (bottom limit), the actual limit of the $t_{overlay}/t_{slab}$ ratio ranged from 0.16 to 0.41, corresponding to an overlay's thickness value ranging from 32 to 82 mm.
3) The values of $t_{overlay}/t_{slab}$ of 0.06, 0.09, 0.12, 0.15, 0.18, 0.21, 0.24, 0.27, 0.30, 0.33, 0.36, 0.39, and 0.42 enhanced the bond's strength by 103 %, 161 %, 190 %, 210 %, 224 %, 233 %, 240 %, 246 %, 251 %, 254 %, 256 %, 259 %, and 263 %, respectively, with regard to the $t_{overlay}/t_{slab}$ of 0.03.
4) The levels of strength degradation of 19 %, 36 %, 51 %, 64 %, and 75 % cause a decrease of 9.9 %, 19.9 %, 29.8 %, 39.8 %, and 49.7, respectively, with regard to 0 % of overlay's level of strength degradation.
5) The specimens that had induced-by-shrinkage stresses at the age of 7 days, 14 days, and 28 days had a degradation by: 8.5 %, 23.4 %, and 41.4 %, respectively, with regard to the 3-day-aged overlay.
6) Making a comparison between the systems with identical thicknesses of overlay and various levels of overlay's strength degradation, the findings showed that the reduction rate in the bond-to-strength ratio was minimal compared to the enhancement rate in $t_{overlay}/t_{slab}$.
7) Guidelines have been introduced to help determine the least value of the overlay's bond strength at a given age, which is needed to make the overlay resist the bond's stresses caused by shrinkage.

5. Future works

The behavior of the concrete overlaying layer was sufficiently studied using different thicknesses where the bond strength at the interface was evaluated. Based on the interesting results of this study, the bond strength of different overlay materials could be studied in the future, considering the effect of reinforcing the layer with different materials.

Data availability statements

The datasets generated and/or analyzed during the current study are available from the corresponding author on reasonable request.

CRediT authorship contribution statement

Rajai Z. Al-Rousan: Writing – review & editing, Writing – original draft, Visualization, Validation, Supervision, Software, Resources, Project administration, Methodology, Investigation, Funding acquisition, Formal analysis, Data curation, Conceptualization. **Bara'a R. Alnemrawi:** Writing – review & editing.

Declaration of competing interest

The authors declare that they have no known competing financial interests or personal relationships that could have appeared to influence the work reported in this paper.

References

[1] L. Teng, K.H. Khayat, Effect of overlay thickness, fiber volume, and shrinkage mitigation on flexural behavior of thin bonded ultra-high-performance concrete overlay slab, Cement Concr. Compos. 134 (2022) 104752, https://doi.org/10.1016/j.cemconcomp.2022.104752.
[2] J. Du, P. Guo, Z. Liu, W. Meng, Highly thixotropic ultra-high-performance concrete (UHPC) as an overlay, Construct. Build. Mater. 366 (2023) 130130, https://doi.org/10.1016/j.conbuildmat.2022.130130.
[3] D. Rambabu, S.K. Sharma, P. Karthik, M.A. Akbar, A review of application of UHPFRC in bridges as an overlay, Innovative Infrastructure Solutions 8 (1) (2023) 57, https://doi.org/10.1007/s41062-022-01030-4.
[4] R.Z. Al-Rousan, B.R. Alnemrawi, The influence of prestress level on the behavior of prefabricated precast concrete bridge deck panel systems with different overlay thicknesses, Structures 58 (2023) 105478, https://doi.org/10.1016/j.istruc.2023.105478.
[5] Y. Zhang, Y.H. Chai, An Analytical model to Evaluate Short- and long-term performances of post-tensioned concrete box-girder bridges rehabilitated by an ultrahigh-performance concrete overlay, J. Bridge Eng. 28 (3) (2023) 04023004, https://doi.org/10.1061/JBENF2.BEENG-5673.
[6] S. Qin, L. Yu, J. Zhang, L. Gao, Fatigue assessment of steel-UHPC composite deck with a thin polymer overlay in a long-span suspension bridge under static and random traffic loads, Int. J. Fatig. 168 (2023) 107409, https://doi.org/10.1016/j.ijfatigue.2022.107409.
[7] U. Attanayake, A.F. Mazumder, Performance-based approach for deciding the age of new concrete for thin epoxy overlay application, Transport. Res. Rec.: J. Transport. Res. Board 2675 (10) (2021) 1055–1068, https://doi.org/10.1177/03611981211014530.
[8] A.F. Mazumder, H. Amunugama, U. Attanayake, Impact of concrete mix ingredients and surface treatments on epoxy overlay performance, Transport. Res. Rec.: J. Transport. Res. Board 2675 (10) (2021) 1161–1173, https://doi.org/10.1177/03611981211014887.
[9] A.F. Mazumder, U. Attanayake, N.S. Berke, Performance of two thin epoxy overlays on new concrete under laboratory and outdoor exposure conditions, Transport. Res. Rec.: J. Transport. Res. Board 2675 (10) (2021) 1406–1419, https://doi.org/10.1177/03611981211016464.
[10] R.Z. Al-Rousan, B.R. Alnemrawi, Interface shear strength prediction of CFRP-strengthened sulfate-damaged shear keys using NLFEA, Int. J. Civ. Eng. 21 (8) (2023) 1385–1402, https://doi.org/10.1007/s40999-023-00829-1.
[11] D.K. Harris, J. Sarkar, T.M. Ahlborn, Characterization of interface bond of ultra-high-performance concrete bridge deck overlays, Transport. Res. Rec.: J. Transport. Res. Board 2240 (1) (2011) 40–49, https://doi.org/10.3141/2240-07.
[12] M.A. Issa, R.Z. Alrousan, Modeling of bond stresses of overlay–bridge deck system, Transport. Res. Rec.: J. Transport. Res. Board 2113 (1) (2009) 72–82, https://doi.org/10.3141/2113-09.
[13] B.R. Alnemrawi, R.Z. Al-Rousan, A.N. Ababneh, The structural behavior of heat-damaged flat slabs with openings of different sizes and locations, Arabian J. Sci. Eng. (2023), https://doi.org/10.1007/s13369-023-08411-6.
[14] R.Z. Al-Rousan, M. Alhassan, M.A. Issa, The optimum overlay thickness of prefabricated full-depth precast concrete bridge deck panel system – 3D non-linear finite element modeling, Eng. Struct. 100 (2015) 264–275, https://doi.org/10.1016/j.engstruct.2015.06.018.
[15] N. Delatte, A. Sehdev, Mechanical properties and durability of bonded-concrete overlays and ultrathin whitetopping concrete, Transport. Res. Rec.: J. Transport. Res. Board 1834 (1) (2003) 16–23, https://doi.org/10.3141/1834–03.
[16] K. Babaei, Evaluation of Concrete Overlays for Bridge Application. Final Report, Research Project Y-3399, Task 2, Washington State Transportation Commission, Federal Highway Administration, 1987 (1987.
[17] A. John, R.D.S. Wells, P. Dimos, Getting better bond in concrete overlays, Concr. Int. 21 (3) (1999) 49–52.
[18] M.M. Sprinkel, Ozyildirim C evaluation of hydraulic cement concrete overlays placed on three pavements in Virginia, Virginia Department of Transportation 2000, 2000. Report No. VTRC01-R2.
[19] K.H. Khayat, W. Meng, K. Vallurupalli, L. Teng, Rheological properties of ultra-high-performance concrete — an overview, Cement Concr. Res. 124 (2019) 105828, https://doi.org/10.1016/j.cemconres.2019.105828.
[20] L. Fan, W. Meng, L. Teng, K.H. Khayat, Effects of lightweight sand and steel fiber contents on the corrosion performance of steel rebar embedded in UHPC, Construct. Build. Mater. 238 (2020) 117709, https://doi.org/10.1016/j.conbuildmat.2019.117709.
[21] Z.B. Haber, J.F. Munoz, I. De la Varga, B.A. Graybeal, Bond characterization of UHPC overlays for concrete bridge decks: laboratory and field testing, Construct. Build. Mater. 190 (2018) 1056–1068, https://doi.org/10.1016/j.conbuildmat.2018.09.167.
[22] M.A. Al-Osta, M.N. Isa, M.H. Baluch, M.K. Rahman, Flexural behavior of reinforced concrete beams strengthened with ultra-high performance fiber reinforced concrete, Construct. Build. Mater. 134 (2017) 279–296, https://doi.org/10.1016/j.conbuildmat.2016.12.094.
[23] M. Pimentel, S. Nunes, Experimental tests on RC beams reinforced with a UHPFRC layer failing in bending and shear, in: Proceedings of the 4th International Symposium on Ultra-high Performance Concrete and High Performance Materials, Kassel, Germany, 2016, pp. 9–11.
[24] L. Hussein, L. Amleh, Structural behavior of ultra-high performance fiber reinforced concrete-normal strength concrete or high strength concrete composite members, Construct. Build. Mater. 93 (2015) 1105–1116, https://doi.org/10.1016/j.conbuildmat.2015.05.030.
[25] H.M. Tanarslan, N. Alver, R. Jahangiri, Ç. Yalçınkaya, H. Yazıcı, Flexural strengthening of RC beams using UHPFRC laminates: bonding techniques and rebar addition, Construct. Build. Mater. 155 (2017) 45–55, https://doi.org/10.1016/j.conbuildmat.2017.08.056.
[26] M. Safdar, T. Matsumoto, K. Kakuma, Flexural behavior of reinforced concrete beams repaired with ultra-high performance fiber reinforced concrete (UHPFRC), Compos. Struct. 157 (2016) 448–460, https://doi.org/10.1016/j.compstruct.2016.09.010.
[27] P.M. Buchanan, D.W. Mokarem, R.E. Weyers, M.M. Sprinkel, Shrinkage of latex-modified and microsilica concrete overlays, Transport. Res. Rec.: J. Transport. Res. Board 1834 (1) (2003) 33–39, https://doi.org/10.3141/1834–05.
[28] O. Bernard, Long Term Behavior of Structural Elements Consisting of Concretes of Different Ages, Pd.D, Swiss Federal Institute of Technology, Lausanne, Switzerland, in French, 2000. Thesis No. 2283.

[29] M.A. Issa, M.A. Alhassan, R. Alrousan, High performance bonded concrete overlays for full-depth and segmental bridge deck construction, in: The PCI National Bridge Conference: Proceedings, October 23–25, 2006, 2006. Grapevine, Texas.
[30] D. Fowler, Stresses in PC Overlays Due to Thermal Changes: A Proposed Design Methodology, University of Texas at Austin, 2004.
[31] R.Z. Alrousan, B.R. Alnemrawi, The behavior of alkali-silica reaction-damaged full-scale concrete bridge deck slabs reinforced with CFRP bars, Results in Engineering 16 (2022) 100651, https://doi.org/10.1016/j.rineng.2022.100651.
[32] ANSYS, ANSYS User's Manual Revision 16.0, ANSYS, Inc., 2016.
[33] K. Willam, E. Warnke, Constitutive model for the triaxial behavior of concrete. International association of bridge and structural engineers, Seminar on concrete structure subjected to triaxial stresses, paper III-1, Bergamo, Italy, May 1974, IABSE Proc 19 (1975), https://doi.org/10.5169/seals-17526.
[34] R. Hawileh, J. Abdalla, M. Tanarslan, Modeling of nonlinear response of r/c shear deficient t-beam subjected to cyclic loading, Comput. Concr. 10 (4) (2012) 419–434, https://doi.org/10.12989/cac.2012.10.4.419.
[35] L. Dahmani, A. Khennane, S. Kaci, Crack identification in reinforced concrete beams using ANSYS software, Strength Mater. 42 (2) (2010) 232–240, https://doi.org/10.1007/s11223-010-9212-6.
[36] Q. Chen, H. Zhang, Y. Zhu, S. Chen, G. Ran, Study on distributions of airflow velocity and convective heat transfer coefficient characterizing duct ventilation in a construction tunnel, Build. Environ. 188 (2021) 107464, https://doi.org/10.1016/j.buildenv.2020.107464.
[37] K.M. Abdalla, R. Al-Rousan, M.A. Alhassan, N.D. Lagaros, Finite-element modelling of concrete-filled steel tube columns wrapped with CFRP, Proceedings of the Institution of Civil Engineers -Structures and Buildings 173 (11) (2020) 844–857, https://doi.org/10.1680/jstbu.19.00011.
[38] Y. Hemmaty, Modeling of the shear force transferred between cracks in reinforced and fiber reinforced concrete structures, in: Proceedings of the ANSYS Conference, 1998, pp. 201–209, 1. Pittsburgh, Pennsylvania, August,.
[39] D.C. Kent, R. Park, Flexural members with confined concrete, J. Struct. Div. 97 (7) (1971) 1969–1990, https://doi.org/10.1061/JSDEAG.0002957.
[40] M. Alhassan, R.Z. Al-Rousan, L.K. Amaireh, M.H. Barfed, Nonlinear finite element analysis of B-C connections: influence of the column axial load, jacket thickness, and fiber dosage, Structures 16 (2018) 50–62, https://doi.org/10.1016/j.istruc.2018.08.011.
[41] R.Z. Al-Rousan, M. Alhassan, R. Al-wadi, Nonlinear finite element analysis of full-scale concrete bridge deck slabs reinforced with FRP bars, Structures 27 (2020) 1820–1831, https://doi.org/10.1016/j.istruc.2020.08.024.
[42] R.Z. Al-Rousan, A. Alkhawaldeh, Numerical simulation of the influence of bond strength degradation on the behavior of reinforced concrete beam-column joints externally strengthened with FRP sheets, Case Stud. Constr. Mater. 15 (2021) e00567, https://doi.org/10.1016/j.cscm.2021.e00567.
[43] M.A. Alhassan, R.Z. Al-Rousan, H.M. Taha, Precise finite element modelling of the bond-slip contact behavior between CFRP composites and concrete, Construct. Build. Mater. 240 (2020) 117943, https://doi.org/10.1016/j.conbuildmat.2019.117943.
[44] N.M.M. Ramos, M.L. Simões, J.M.P.Q. Delgado, V.P. de Freitas, Reliability of the pull-off test for in situ evaluation of adhesion strength, Construct. Build. Mater. 31 (2012) 86–93, https://doi.org/10.1016/j.conbuildmat.2011.12.097.
[45] E. Bonaldo, J.A.O. Barros, P.B. Lourenço, Bond characterization between concrete substrate and repairing SFRC using pull-off testing, Int. J. Adhesion Adhes. 25 (6) (2005) 463–474, https://doi.org/10.1016/j.ijadhadh.2005.01.002.
[46] Y. Liu, Z. Qian, Y. Yin, H. Ren, Investigation on interlayer behaviors of a double-layered heterogeneous asphalt pavement structure for steel bridge deck, J. Mater. Civ. Eng. 34 (5) (2022) 04022062, https://doi.org/10.1061/(ASCE)MT.1943-5533.0004206.
[47] J. Carlswärd, Shrinkage Cracking of Steel Fibre Reinforced Self Compacting Concrete Overlays: Test Methods and Theoretical Modelling: Test Methods and Theoretical Modelling, Luleå University of Technology, Sweden, 2006. Ph.D. Thesis.
[48] S. Hak-Chul, A.L. David, Effects of shrinkage and temperature in bonded concrete overlays, ACI Mater. J. 101 (5) (2004) 358–364, https://doi.org/10.14359/13421.
[49] M.A. Issa, Evaluation and recommendation of overlay materials for the new Mississippi river bridge, Final Report, Illinois Department of Transportation, 2004.